Terahertz scattering from granular material

Lisa M. Zurk,[1,*] **Brian Orlowski,**[1] **Dale P. Winebrenner,**[2] **Eric I. Thorsos,**[2] **Megan R. Leahy-Hoppa,**[3] **and L. Michael Hayden**[3]

[1]*Department of Electrical and Computer Engineering, Portland State University, Portland, Oregon 97207, USA*
[2]*Applied Physics Laboratory, University of Washington, Seattle, Washington 98195, USA*
[3]*Department of Physics University of Maryland Baltimore County, Baltimore, Maryland 21250, USA*
*Corresponding author: zurkl@cecs.pdx.edu

Terahertz (THz) imaging is emerging as a potentially powerful method of detecting explosive devices, even in the presence of occluding materials. However, the characteristic spectral signatures of pure explosive materials may be altered or obscured by electromagnetic scattering caused by their granular nature. This paper presents THz transmission measurements of granular systems representative of explosives and presents results from dense media theory that accurately explain the observed scattering response. © 2007 Optical Society of America

OCIS codes: 290.0290, 300.0300.

1. INTRODUCTION

Recent advances in ultrafast optical laser technology have improved generation and detection of energy within the terahertz (THz) portion of the electromagnetic (EM) spectrum [1–4]. One particularly promising sensor application is the use of THz spectroscopy to detect the presence of explosive materials. Initial measurements [5–9] indicate that explosives may have unique spectral characteristics in this region and these characteristics provide a discernible "fingerprint." The fingerprint differs from that of many common obscuring materials (e.g., paper, plastic, and cloth), which have a relatively flat spectral response [10].

A potential complication to spectroscopic identification of explosives is internal dielectric heterogeneity, particularly in the case of plastic explosives. Common plastic explosives consist of explosive crystals embedded in plastic filler (see, as an example, Fig. 1), the latter typically comprising 5%–20% of total volume. The real parts of permittivities of crystalline explosive grains and plastic fillers are not well known, but are thought to differ substantially; this may lead to substantial internal scattering from dielectric heterogeneities. In addition, micron-scale air voids, which (typically) occupy a few percent of the volume of explosive material, occur both within and outside explosive crystal grains, and are a necessary feature of explosive materials [12,13]. Air voids are a second source of potentially significant dielectric heterogeneity. For both the explosive grains and the air voids, the size and density of the inclusions can significantly vary as a result of the manufacturing process and desired parameters of the explosive (e.g., sensitivity versus detonation efficiency).

From a spectroscopic perspective, the presence of discrete scatterers produces classical EM scattering that may obscure spectral features characteristic of chemical composition. Thus there are two critical questions for applications in explosive detection: First, does significant energy in the THz wave field in explosive granular systems (or, more generally, in granular systems with dimensions and grain/background permittivity contrasts similar to those in plastic explosive devices) remain in the mean, coherent field (even though particle sizes are comparable to the wavelength), or is most of the energy scattered incoherently? And second, what theoretical methods yield accurate approximations to the observed fields?

Here we address these questions using measurements and modeling of THz transmission through pressed pellets of granular polyethylene (PE) with varying grain sizes and thicknesses. Granular PE is commonly used as an embedding material for small quantities of crystalline explosives with a similar grain size for the measurement of spectral transmission [10]. Moreover, the contrast between the real parts of permittivity of PE grains and air is comparable to that between crystalline grains of explosive and common plastic binders, while dielectric absorption in PE is much less than that in explosives [10]. Incoherent scattering in pressed, granular PE, therefore serves as a likely upper bound on that in similar volumes of plastic explosives, and accurate theory for the coherent field in our model system will apply to plastic explosive systems as well.

To model the coherent THz field, a dense medium model was applied to calculate an effective wave number within the quasi-crystalline approximation (QCA) [14]. QCA is an analytic formulation (i.e., a formally averaged formulation) that accounts for the multiple scattering between densely packed dielectric particles, and has been applied previously to a variety of applications such as remote sensing of snow [15–17], scattering in photonic crystals [18], and dense media experiments [19].

This paper is organized as follows. The next section describes the experimental setup and procedure used to obtain the transmission measurements for PE. A description is then given of the QCA scattering formulation and geometric model for the PE system. This is followed by a comparison between experimental and theoretical results.
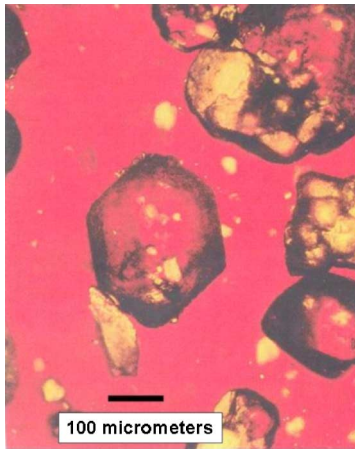
Fig. 1.   (Color online) Photomicrograph of a plastic explosive sample showing 150-micron HMX crystals in a plastic filler [11].

2. THz MEASUREMENTS

Terahertz time-domain spectroscopy of transmission through four pellets of compressed PE powder was conducted in the Laboratory for Nonlinear Optical Studies of Macromolecular Photonic Materials at the University of Maryland, Baltimore County. The spectrometer performed optical rectification of femtosecond, infrared laser pulses by an electro-optic polymer material [1,2,20] to produce short pulses of energy at frequencies from 0.5–8 THz. The experimental setup is shown in Fig 2.

The pellets were fabricated from two different manufacturing lots of spectrophotometric-grade PE power (Sigma-Aldrich, St. Louis, Mo.), one in which the sizes of PE grains were relatively small (approximately 20 μm in radius, cf. Fig. 3), the other in which grains were larger, approximately 60 μm in radius. The pellets each contained 25–60 mg of PE powder compressed into disks of thickness 0.77 mm for the small size and 1.82 mm for the larger size (in a hand press at pressures of roughly 16,000 psi).

The electric field of each pulse after transmission was detected electro-optically. The magnitude of the Fourier transform of the detected electric field is shown in Fig. 4 for three cases—one with no pellet in the spectrometer and two pellets composed of powder with differing grain sizes.

In analyzing these results, we assume that wavefronts of the illuminating THz field were planar over the extent
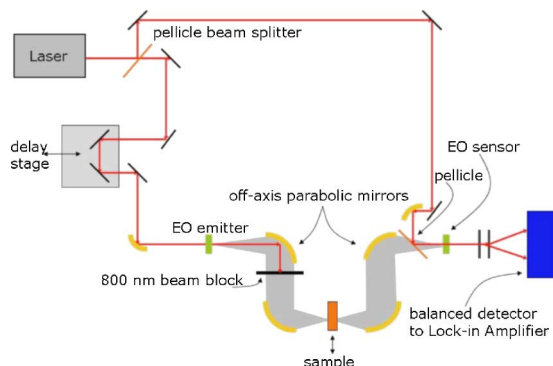

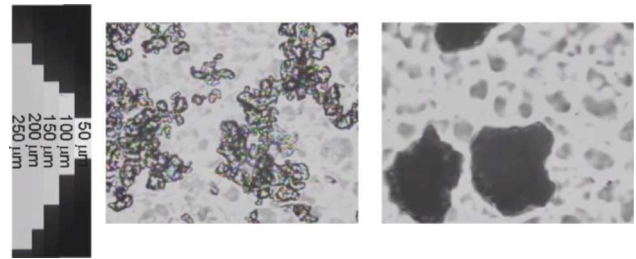Fig. 2.   (Color online) Experimental setup for THz spectroscopy.

Fig. 3.   (Color online) Pictomicrographs of two different manufacturer lots of PE samples showing different grain sizes. Sample on left is termed SGPE and right-hand sample is LGPE. The scale in μm is shown in the far left.

of each pellet, and that the transmitted wavefronts were detected in the far-field and thus were also planar, so that plane-wave transmission coefficients are appropriate to describe the data. Moreover, we assume that averages over small intervals of bandwidth in the transmission spectrum effectively yield averages over configurations of particle positions in the powder samples [21], so that the data can be compared with theoretical expressions for transmission of the coherent field through random media.

3. DENSE MEDIUM SCATTERING CALCULATIONS

Understanding wave propagation in systems of discrete, particulate scatterers is important for a wide variety of applications and has thus been widely studied. In contrast to many cases in optics, the situation considered in this paper involves scatterers which are comparable in size to the radiation wavelength, occupy more than a few percent of the volume, and whose refractive index may differ strongly from that of the material in which they are embedded. Under these conditions, multiple scattering between the particles can be a significant effect and thus the application of dense media theory [14] is necessary.
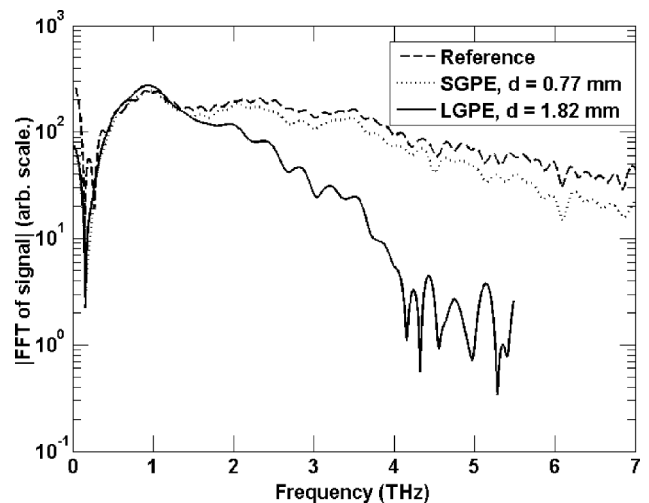

Fig. 4.   Magnitude of the Fourier transform of the measured transmission signal for the PE samples shown in the previous figure. Note significantly greater attenuation for LGPE sample at higher frequencies. Pellet thickness was 0.77 and 1.82 mm for SGPE and LGPE samples, respectively. For this and subsequent plots the data curves are truncated once they reach the estimated noise floor.

We use the QCA formulation, based on the configurational average of the Foldy–Lax multiple scattering equations, to model the mean (coherent) field. A brief overview of QCA is provided here; further details can be found in [14].

Consider a system of N identical dielectric scatterers at positions $\bar{r}_l, l = 1 \cdots N$, with relative permittivity ϵ_s, embedded in a background medium of relative permittivity ϵ_b. The particles are subject to an incident electric field $\bar{E}^{inc}(\bar{r})$ at frequency ω which can be written in terms of the regular vector spherical wave functions $\bar{M}_{mn}^{(1)}$ and $\bar{N}_{mn}^{(1)}$ (the superscript denotes the choice of wave functions that are regular at the origin [22]) as

$$\bar{E}^{inc}(\bar{r}) = \sum_{m,n} [a_{mn}^{(M)} \bar{M}_{mn}^{(1)}(kr, \theta, \phi) + a_{mn}^{(N)} \bar{N}_{mn}^{(1)}(kr, \theta, \phi)], \quad (1)$$

where $a_{mn}^{(M)}$ and $a_{mn}^{(N)}$ are the (known) coefficients of the spherical wave functions and k is the background wave number, $k = \sqrt{\epsilon_b}\omega/c$, with c defined as the speed of light in free space.

The field exciting the lth particle is due to both the incident field and the field (multiply) scattered from all the other particles, and can be written in terms of spherical wave harmonics as

$$\bar{E}_l^{ex}(\bar{r}) = \sum_{m,n} [w_{mn}^{(M)} \bar{M}_{mn}^{(1)}(kr, \theta, \phi) + w_{mn}^{(N)} \bar{N}_{mn}^{(1)}(kr, \theta, \phi)], \quad (2)$$

where $w_{mn}^{(M)}$ and $w_{mn}^{(N)}$ are now unknown coefficients to be determined. These coefficients can be grouped into a vector of length $2L_{max} = 2n_{max}(n_{max}+2)$, ($n_{max}$ is the number of multipoles retained in the electric and magnetic multipole expansion) and written in a matrix form as

$$\bar{w}^{(l)} = \sum_{j=1, j \neq l}^{N} \bar{\bar{\sigma}}(k\bar{r}_{lj})\bar{\bar{T}}\bar{w}^{(j)} + e^{i\bar{k}_i \cdot \bar{r}_l}\bar{a}_{inc}, \quad (3)$$

where $\bar{a}_{inc}$ is a vector of the incident field coefficients, $\bar{\bar{\sigma}}(k\bar{r})$ is a $2L_{max} \times 2L_{max}$ matrix of terms accounting for a coordinate transformation, $\bar{r}_{lj} = \bar{r}_j - \bar{r}_l$ is the vector pointing from the center of the lth particle to the center of the jth particle, and $\bar{\bar{T}}$ is the T-matrix for the particles. The physical interpretation of Eq. (3) is that the excitation for the lth particle in the system is a combination of the incident wave and the waves scattered from all the other ($j = 1 \cdots N, j \neq l$) particles in the system.

Once $\bar{w}^{(l)}$ is determined, the scattered field coefficients can be computed using

$$\bar{a}^{S(l)} = \bar{\bar{T}}\bar{w}^{(l)}. \quad (4)$$

Note that the above equations are a rigorous expression for the scattered field that includes all orders of multiple scattering. However, the terms (1) and (2) depend on the exact position and nature (shape, orientation, etc.) of the particles; and are thus difficult to solve exactly for most practical problems. For some problems, an iterative numerical approach can be employed [15] with Monte Carlo averaging over multiple realizations.

An alternate, analytical approach is to perform statistical configurational averaging using conditional averaging. Denoting the conditional probability function for the random particle position as $p(\bar{r}_1, \bar{r}_2 \cdots \bar{r}_l' \cdots \bar{r}_N | \bar{r}_l)$ (where $'$ denotes that term is absent) the conditional average can be written as

$$\mathcal{E}_l(\bar{w}^{(l)}) = \int d\bar{r}_1 d\bar{r}_2 \cdots d\bar{r}_l' \cdots d\bar{r}_N \bar{w}^{(l)} p(\bar{r}_1, \bar{r}_2 \cdots \bar{r}_l' \cdots \bar{r}_N | \bar{r}_l),$$

$$= \bar{w}(\bar{r}_l), \quad (5)$$

where $\mathcal{E}_l(\cdot)$ denotes the expected value given the position and state of the lth particle. The conditional probability can be written using Bayes' rule to generate a hierarchy of equations. The QCA truncates the resulting equation at the bivariate level. For identical particles in a statistically homogeneous medium this produces

$$\bar{w}(\bar{r}_l) = n_0 \int d\bar{r}_j g(|\bar{r}_j - \bar{r}_l|)\bar{\bar{\sigma}}(k\bar{r}_{lj})\bar{\bar{T}}\bar{w}(\bar{r}_j) + e^{i\bar{k}_i \cdot \bar{r}_l}\bar{a}_{inc}, \quad (6)$$

where n_0 is the number of particles per unit volume and $g(r)$ is the pair distribution function for a two particle separation distance of r. To determine the effective permittivity, we use the approach presented in [14] that is briefly described here.

An approximate solution is assumed that represents the scattered wave in terms of an effective wave number $K_{eff} = \sqrt{\epsilon_{eff}}\omega/c$:

$$\bar{w}(\bar{r}_l) = \bar{a}_{inc}e^{i\bar{K}_{eff}\cdot\bar{r}_l}, \quad (7)$$

with an incident field given by $\bar{E}^{inc}(\bar{r}) = \hat{y}e^{ikz}$ and the corresponding spherical wave expansion in Eq. (1). The expression in Eq. (7) is then inserted into Eq. (6), and terms with the effective wavenumber K_{eff} are balanced to satisfy a generalized Lorentz–Lorenz law. Then the Ewald–Oseen extinction theorem is used to balance the integral equation for waves traveling with the background wave number k. Physically, this ensures that the medium generates a wave that extinguishes the incident wave. This process yields a single scalar equation in the form of the Ewald–Oseen extinction theorem:

$$K_{eff} - k = -\frac{\pi i n_0}{k^2} \sum_n (T_n^{(M)} X_n^M + T_n^{(N)} X_N^{(N)})(2n + 1), \quad (8)$$

where $T_n^{(M)}$ and $T_n^{(N)}$, given in [14], are components of the T-matrix (only the $m = \pm 1$ terms are nonzero for the choice of incident field, and are included in the above). In Eq. (8), X_n^M and X_n^N are unknown amplitudes that satisfy a system of simultaneous equations resulting from the Lorentz–Lorenz law (see [14] for full details). In general, a closed form solution can only be obtained in the low-frequency limit. For larger values of ka, the solution can be determined numerically. For a nontrivial solution the determinant of the coefficients for the system of simultaneous equations must vanish, yielding an equation for the effective wave number in terms of the background wave number and scattering coefficients. One approach to solve this equation is to search for the roots of the determinant (in the complex K_{eff} plane) using Muller's method. The initial guesses are obtained from 1) Foldy's approximation (i.e., valid for sparse concentrations), and 2) the low-frequency solution.

The QCA solution depends on the probabilistic particle placement within the volume. For statistically isotropic media, the random placement of the particles can be represented by the Percus Yevick (PY) pair distribution function [14].

4. RANDOM MEDIA MODEL

In the present work, QCA is used to determine the effective wave number, K_{eff}, of the PE pellets. By definition, the effective wave number is the wave number for an equivalent, homogeneous material whose propagation characteristics (including the attenuation due to absorption and scattering) is equal to that of the random media. As described previously, the PE grains were compressed into pellets with resulting fractional volumes of approximately 80%. The random media model that was used to model this composite material is a "Swiss cheese" model, where the remaining 20% of the volume is modeled as spherical air voids that are present in a background of PE (relative permittivity of the PE is $\epsilon = 2.13$). Figure 5 shows an illustration of the random media model for the PE pellet.

In a cube filled with single size spheres, even dense packing will create void spaces between the spheres. The voids that are between the spheres will provide dielectric contrast, and can be viewed as the scatterers (in a homogeneous background) that contribute to the overall scattering of the entire system. Although the void shape would, in general, be nonspherical, it will be modeled as a sphere with an equivalent volume. For simplicity, a model of single size spheres at densest packing is used to estimate the size of equivalent void volume spheres. Such a model yields a 26% void volume, and the number of equivalent spherical voids is adjusted to yield the known 20% void volume for the PE samples. The densest packing results in a configuration where three spheres are set in the shape of a triangle, and a single sphere is placed on top of them. A line can be drawn from center to center of all of the spheres and will create a tetrahedron, as shown in Fig. 6 (adapted from [23]).

The following equations are used to calculate the extragranular void volume that exists within the tetrahedron:
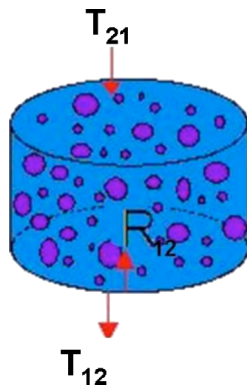

Fig. 5. (Color online) Random media model used in QCA calculations. Background is modeled as pure PE with a relative permittivity of 2.13. Air voids occupy 20% by volume, and have a radius of either 8 or 24 μm, for SGPE and LGPE, respectively.

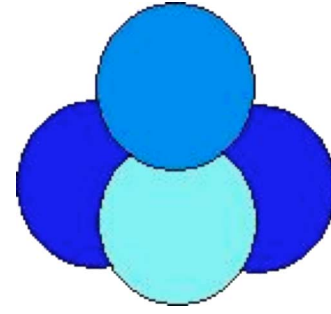

Fig. 6. (Color online) Close packing of spheres with tetrahedron center.

$$V = \frac{\sqrt{2}l^3}{12} = \frac{2\sqrt{2}r^3}{3}, \qquad (9)$$

where $l = 2r$ denotes the side of the tetrahedron and r is the radius of the PE grains.

To find an approximation for the volume of the sphere pieces inscribed in the volume, the problem is transformed to spherical coordinates, and after some geometry the following triple integral is produced:

$$\int_0^r \int_0^{\pi/3} \int_0^{\pi/3} (r')^2 \sin(\theta) \, d\theta \, d\phi \, dr' = \pi r^3/18. \qquad (10)$$

There are four of these sphere pieces, therefore the total PE volume is $2\pi r^3/9$.

Subtracting the PE volume from the tetrahedron volume and equating the residual to the volume of an equivalent spherical void, the void radius, r_v, is found to be

$$r_v = \left[\frac{1}{\sqrt{2}\pi} - \frac{1}{6} \right]^{1/3} r. \qquad (11)$$

The size of these voids is computed by considering a dense packing of PE spheres and computing the equivalent sphere volume for the remaining air gaps. For the small grain PE (SGPE) and large grain PE (LGPE) samples this gives a void radius of $r_v = 8$, and 24 μm, respectively. Note that in the terahertz region, these spherical scatterers are in the Mie regime, which means that low frequency Rayleigh scattering does not apply, which in turn leads to the requirement for multipole expansions, even in the case of spherical scatterers.

The expression for the effective wave number also depends on the particle placement within the volume. For statistically isotropic media, the random placement of the particles can be represented by the PY pair distribution function [14].

5. COMPARISON OF DATA AND THEORY

The experiments measured the transmission through pellets comprised of PE with air voids (see Fig. 5). The effective wave numbers for these media were computed with QCA over the range of $1-12$ THz to yield an attenuation coefficient $\alpha = \text{Im}(K_{eff})$. Note that this attenuation is due entirely to scattering from the PE grains, since the intrinsic attenuation within the grains has been neglected. In

addition to losses within the pellet, losses occurred at the two approximately planar interfaces. These are modeled as planar with T_{jk} and R_{jk} as the normal incidence Fresnel transmission and reflection coefficients from the kth medium to the jth medium, respectively, as shown in Fig. 5. The Fresnel coefficients are calculated from the QCA effective wave number, K_{eff}, as

$$T_{21} = \frac{2k_0}{k_0 + K_{eff}}, \quad T_{12} = \frac{2K_{eff}}{k_0 + K_{eff}}, \tag{12}$$

and

$$R_{12} = \frac{K_{eff} - k_0}{K_{eff} + k_0}, \tag{13}$$

where k_0 is the wave number in free space. The transmitted field in the frequency domain, E, can then be estimated for a slab of thickness d, and accounting for all orders of multiple reflections by

$$E = \frac{T_{21}T_{12}e^{-\alpha d}}{1 - R_{12}^2 e^{-2\alpha d}} E_{REF}, \tag{14}$$

where E_{REF} is a reference field value accounting for the spectral variation of the measurement system.

The simulated field calculated as described above is shown in Fig. 7 with the previously presented measured data. As shown in Fig. 7, the scattering calculation successfully explains the large differences in the transmitted field for these two different PE samples.

It should be noted that the LGPE and SGPE measurements were made with different pellet thicknesses (d =1.82 mm and d=0.77 mm, respectively). To remove the influence of varying thicknesses, the measured data were inverted by solving Eq. (14) for α to determine a frequency-dependent attenuation. This is plotted in Fig. 8 along with the predicted attenuation coefficient from the QCA calculation (dashed lines). While small details of the attenuation are not captured by the simulation, clearly

Fig. 8. Attenuation coefficient for measurements and simulations from QCA theory (shown with markers) for LGPE (solid line) and for SGPE (dotted line).

the trends for the two media are captured, showing the important effect of grain size on attenuation.

Further results are shown in Fig. 9 for measurements of large grain PE with pellet thicknesses of 1.42 and 3.22 mm. Also shown are additional random media calculations obtained in the same fashion as described above, and good agreement is obtained with measured values.

6. CONCLUSIONS AND FUTURE WORK

Terahertz spectroscopy is a promising technique for the detection and identification of explosive materials. The identification is based on the strong spectral signatures produced by pure explosive material. However, actual explosive materials are a composite mixture of explosive grains with plastic fillers and air voids. This granular nature produces strong classical (EM) scattering in the THz region.

To explore the grain-dependent scattering physics, this paper presents experimental measurements of PE samples acquired from two different manufacture bins. Although the samples had the same chemical composition and were within manufacturer tolerances, they produced
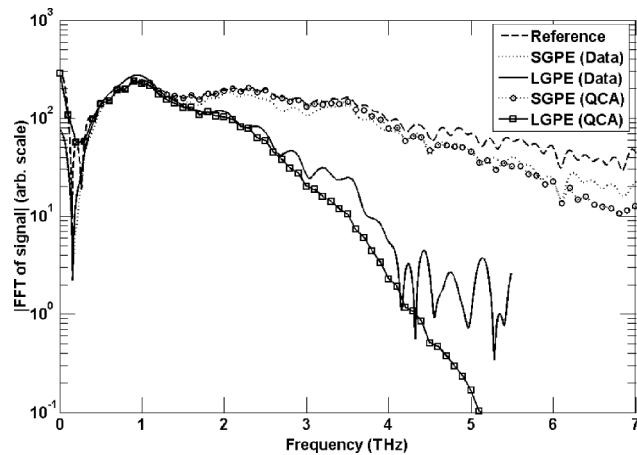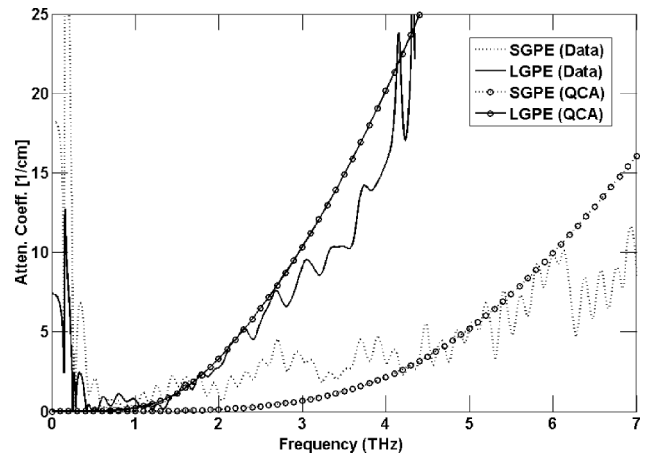

Fig. 7. Magnitude of the Fourier transform of the measured transmission signal for LGPE (solid) and SGPE (dotted). Background is modeled as pure PE with a relative permittivity of 2.13. Air voids occupy 20% by volume, and have a radius of either 8 or 24 μm, for SGPE and LGPE, respectively. Calculations for QCA shown as open square (LGPE) and open circle (SGPE) markers.
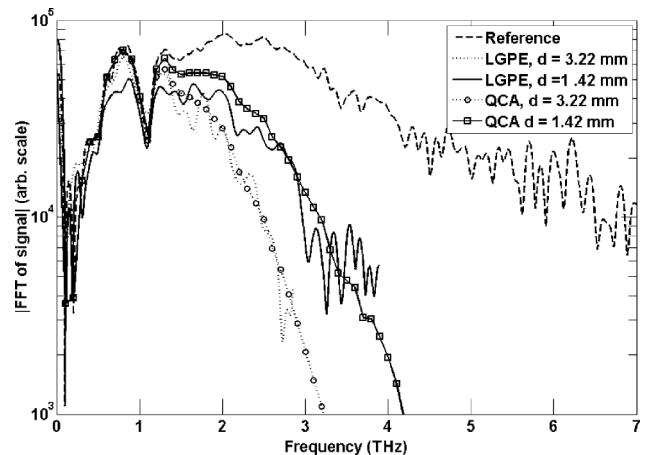

Fig. 9. Additional measurements of LGPE samples with pellet thicknesses of 1.42 and 3.22 mm. Calculations with QCA shown with markers.

markedly different THz scattering responses. Examination of the samples indicated that one sample had much larger grain sizes, and these larger particles produced increased attenuation.

The experimental results have transmission spectra whose properties are similar to those produced by applying the quasi-crystalline approximation (QCA), a dense media scattering formulation. An effective wave number was calculated using QCA for a mixture of PE and air voids. The imaginary part of this wave number, which represented the amount of wave extinction due to scattering from the air voids, was used to explain the transmitted electric field observed in the measurements.

The results in this paper indicate a strong dependence of the THz scattering on the microstructure of the sample material. This appears to be true for the PE samples considered in this paper, and may also apply to other materials such as foams and porous ceramics. Future investigation is needed to understand the effect for more lossy materials.

For the PE samples the EM scattering introduced an attenuation that increased with frequency at a rate dependent on the particle size. This scattering response would effect the THz spectra by introducing a frequency roll-off that is sensitive to the microstructure of the material, and thus has the potential of modulating the spectra in a manner dependent on the class of explosive. For more complicated materials the effect on the THz signature may be more severe, and a scattering model would be useful to understand the dependence on the crystalline structure and orientation of the grains. For the results discussed in this paper, an analytic dense media formulation was adequate to explain the observed results. Future work will entail the construction of dense media models for explosive mixtures, and the further development of dense media theory to explain transmission and reflection spectroscopy from these mixtures.

ACKNOWLEDGMENTS

REFERENCES

1. L. M. Hayden, A. M. Sinyukov, M. R. Leahy, J. French, P. Lindahl, W. N. Herman, R. J. Tweig, and M. He, "New materials for optical rectification and electrooptic sampling of ultrashort pulses in the terahertz regime," J. Polym. Sci., Part B: Polym. Phys. **41**, 2492–2500 (2003).
2. A. M. Sinyukov and L. M. Hayden, "Efficient electrooptic polymers for THz applications," J. Phys. Chem. B **108**, 8515–8522 (2004).
3. X. Zheng, A. Sinyukov, and L. M. Hayden, "Broadband and gap-free response of a terahertz system based on a poled polymer emitter-sensor pair," Appl. Phys. Lett. **87**, 081115 (2005).
4. M. Tonouchi, "Cutting-edge terahertz technology," Nat. Photonics **V1**, 97–105 (2007).
5. M. C. Kemp, P. F. Taday, B. E. Cole, J. A. Cluff, A. J. Fitzgerald, and W. R. Tribe, "Security applications of terahertz technology," Proc. SPIE **5070**, 44–52 (2003).
6. K. Yamamoto, M. Yamaguchi, F. Miyamaru, M. Tani, M. Hangyo, T. Ikeda, A. Masushita, K. Koide, M. Tatsuno, and Y. Minami, "Noninvasive inspection of C-4 explosive in mails by terahertz time-domain spectroscopy," Jpn. J. Appl. Phys., Part 2 **43**, L414–L417 (2004).
7. F. Huang, B. Schulkin, H. Altan, J. F. Federici, D. Gary, R. Barat, D. Zimdars, M. Chen, and D. B. Tanner, "Terahertz study of 1,3,5-trinitro-s-triazine by time-domain and Fourier transform infrared spectroscopy," Appl. Phys. Lett. **85**, 5535–5537 (2004).
8. J. Barber, D. E. Hooks, D. J. Funk, R. D. Averitt, A. J. Taylor, and D. Babikov, "Temperature-dependent far-infrared spectra of single crystals of high explosives using terahertz time-domain spectroscopy," J. Phys. Chem. A **109**, 3501–3505 (2005).
9. M. R. Leahy-Hoppa, M. J. Fitch, X. Zhang, L. M. Hayden, R. Osiander, "Wideband terahertz spectroscopy of explosives," Chem. Phys. Lett. **434**, 227–230 (2007).
10. W. R. Tribe, D. A. Newham, P. F. Taday, and M. C. Kemp, "Hidden object detection: Security applications of THz technology," Proc. SPIE **5354** 168–176 (2004).
11. J. E. Reagh, "Checking out the hot spots," *Science and Technology Review* (Lawrence Livermore National Laboratory, 2003).
12. J. E. Reagh, "Grain-scale dynamics in explosives," Technical Report No. ID-150388 (Lawrence Livermore National Laboratory 2002).
13. L. Borne and A. Beaucamp, "Effects of crystal internal defects on projectile impact initiation," French-German Research Institute of Saint-Louis (ISL), P.O. Box 34 - F 68301 Saint-Louis Cedex.
14. L. Tsang, J. A. Kong, and K. H. Ding, *Scattering of Electromagnetic Waves, Theories, and Applications* (Wiley, 2000).
15. L. M. Zurk, L. Tsang, K. H. Ding, and D. P. Winebrenner, "Monte Carlo simulations of the extinction rate of densely packed spheres with clustered and nonclustered geometries," J. Opt. Soc. Am. **12**, 1772–1781 (1995).
16. L. M. Zurk, L. Tsang, J. Shi, and R. Davis, "Electromagnetic scattering calculated from pair distribution functions retrieved from planar snow sections," IEEE Trans. Geosci. Remote Sens. **35**, 1419–1428 (1997).
17. L. Tsang, C. Chen, A. Change, J. Guo, and K. Ding, "Dense media radiative transfer theory based on quasicrystalline approximation with applications to passive microwave remote sensing of snow," Radio Sci. **35**, 731–749 (2000).
18. A. Ponavina, S. Kachan, and N. Silvanovich, "Statistical theory of multiple scattering of waves applied to three-dimensional layered photonic crystals," J. Opt. Soc. Am. B **21**, 1866–1875 (2004).
19. Y. Kuga, D. Rice, and R. D. West, "Propagation constant and the velocity of the coherent wave in a dense strongly scattering medium," IEEE Trans. Antennas Propag. **44**, 326–332 (1996).
20. X.-C. Zhang, X. F. Ma, Y. Jin, T.-M. Lu, E. P. Boden, P. D. Phelps, K. R. Stewart, and C. P. Yakymyshyn, "Terahertz optical rectification from a nonlinear organic crystal," Appl. Phys. Lett. **61**, 3080–3082 (1992).
21. F. T. Ulaby, R. K. Moore, and A. K. Fung, *Microwave Remote Sensing* (Addison-Wesley, 1982).
22. J. A. Stratton, *Electromagnetic Theory* (McGraw-Hill, 1941).
23. F. Jackson and E. W. Weisstein, "Tetrahedron," http://mathworld.wolfram.com/tetrahedron.html.